COMPUTED TOMOGRAPHY FOR NON-DESTRUCTIVE INSPECTION OF HOT STRUCTURES AND TPS COMPONENTS

Thomas Ullmann, Raouf Jemmali, Severin Hofmann, Thomas Reimer, Christian Zuber, Kornelia Stubicar and Hendrik Weihs

German Aerospace Center (DLR)
Institute of Structures and Design, Pfaffenwaldring 38-40, 70569 Stuttgart (Germany)
For correspondence: Thomas.Ullmann@dlr.de

ABSTRACT

Verifying the quality of a large TPS structure component's material and therefore providing its flight readiness capability, belongs to one of the most challenging objectives for non-destructive evaluation techniques. Especially when different components of fibre ceramic composites are joined together or attached to other parts of differing materials (e.g. bulk ceramics, metals, insulations, seal elements), it is always of great interest to obtain proper information about the interfaces between these parts. Well known and approved NDE methods such as radiography, ultrasound inspection or lock-in thermography only offer a two-dimensional view of a three-dimensional structure with a projection of all detectable features through the structure's thickness. This gives way to sometimes quite distinct interpretations of microstructural features and defects. Furthermore, some of these inspection techniques do not allow to scan structural components without using a coupling media such as water or at least a contact gel as used with ultrasound transducers. Other NDE techniques are not suitable to inspect special regions which are located at inaccessible areas as for example the inner side of a curved structure with joined stiffeners as reinforcement elements. Sometimes it is just the penetration depth that is not sufficient to get the necessary information of failure critical areas. However, with X-ray based computed tomography (CT), non-destructive evaluation will be enforced with a powerful tool that provides three-dimensional data with exceptional high resolution. CT inspections allow the detection of flaws such as microcracks, voids and porosity distributions in the microstructure and joining interfaces between different structure components in every part of the structure's volume.
Eight years ago, DLR was successfully using computed tomography for the first time to prove the good quality of the joining interfaces between the X-38 nose cap structure and its CMC load introduction attachments. Because there was no CT available at that time, it was decided to use a medical CT facility at a hospital nearby. Though it was not possible to obtain images of a higher resolution, the interfaces of the outer CMC shell (nose cap) and each load introduction attachment or pressure port plug was inspected in detail. In the meantime, DLR is operating its own CT test facilities for systematic non-destructive material inspections. In the following it is shown how the large CT facility v|tome|x L450 was successfully used for an in-situ evaluation of the load introduction attachments of EXPERT's CMC nose cap structure.

INTRODUCTION

With ongoing developments in high performance CMC structure designs, non-destructive inspection (NDI) technology is going to play a more and more important role. For the purpose of quality assurance, the prime objective of NDI is the detection and identification of material flaws that could lead to impairments of the functionality of structure components. But furthermore it is necessary to evaluate and classify all kinds of microstructural features in order to separate those which are known as harmless or at least non relevant for application purposes from those which are considered to be precarious for the structure component under load. Attaining this goal means to consider design aspects as well because the anisotropic microstructure of CMC materials and the joining interfaces between different structure elements may create specific conditions for the initiation of critical stresses which may encourage the occurrence and propagation of larger defects (e.g. macroscopic cracks or delaminations). To understand the propagation of material and structure relevant defects, it is inevitable to go both ways of experimental testing with demonstrators or full integrated structure components and simulating load cases with numerical modelling. The difficulty is to obtain the full data set from experimental testing and to consider all relevant boundary conditions for the development of a reliable defect propagation simulation model which is capable to predict material and structural failure under realistic load conditions. Non-destructive inspection with computed tomography (CT) provides the opportunity of monitoring the entire structural information of a tested CMC component and to transfer the data digitally to a finite element simulation. Hence, with systematic CT investigations it is possible to study the initiation and propagation of material defects under structural aspects to the point of component failure. The identification and quantitative classification of material defects and failure critical design elements of structure components as part of a quality assurance system is the fundamental basis of a reliable live prediction model for CMC structures in the future.

CT TEST FACILITIES AT DLR

Since January 2008, DLR is operating two CT test facilities at the research centre in Stuttgart. With the v|tome|x L450 facility (Fig. 1), it is possible to scan large structure components. The maximum scanning range is up to 800 mm in width and 1100 mm in height. The CT facility is provided with two X-ray sources: the 240 kV microfocus and the 450 kV high power minifocus tube which are basically differing in the size of the focal spot diameter. The pixel size of the flat panel detector array is 200 µm. Like a digital image is composed of a two-dimensional matrix of numerous small dots (pixels), a CT scan is consisting of a three-dimensional cloud of numerous dots (with up to ≥ 65000 different grey values) that are so to say volume pixels or just "voxels". With a focal spot diameter of 3 × 5 µm (microfocus), it is possible to attain a minimum voxel size of approximately 5 µm. The voxel size *V* is given by:

$$V = \frac{P}{M} = P \cdot \frac{FOD}{FDD} \tag{1}$$

Where *P* is the detector's pixel size, *M* is the geometric magnification which is the ratio of the focus-detector distance (*FDD*) and the focus-object (specimen) distance (*FOD*). The measurement configuration is depicted in Figure 2 below. An object that is inspected by CT has to be penetrated by X-radiation in any direction and its diameter *d* or at least the diameter of the ROI[1] must not exceed the size of the effective detector area. In general there is one rule: the smaller the specimen's rotation body diameter *d*, the higher is the attainable resolution.

Fig. 1. Large CT test facility with the C/C-SiC nose cap structure of EXPERT mounted inside (DLR Stuttgart)

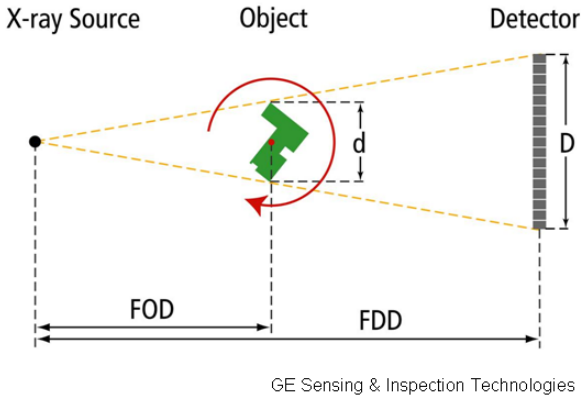

Fig. 2. Schematic measurement configuration of a computed tomography scan

The second CT test facility at DLR is provided with a 180 kV X-ray tube of different design which is capable to generate a focal spot diameter of less than 1 µm. With the so called Nanotome CT facility it is possible to perform high resolution CT scans with a minimum voxel size of approximately 600 nm. However, this is only possible if the dimension of the specimen is not exceeding 2 mm in length of the edge. The Nanotome facility is suitable to inspect microstructural details of small specimens.

CT INSPECTION OF CMC COMPONENTS

First Efforts on using CT Technology for CMC Component Inspection

About ten years ago, the CMC nose cap structure of the X-38 reentry vehicle was designed and manufactured at DLR. The whole nose assembly – including the chin panel, the CMC nose skirts and a full set of US made insulation tiles – was fully integrated, tested and qualified as flight hardware according to NASA standards (Fig. 3) [1,2]. The C/C-SiC nose cap structure was manufactured by using the liquid silicon infiltration process (LSI) which was developed and established at DLR's Institute of Structures and Design before [3]. The C/C-SiC shell was provided with eight anchorage points at the interior side (Fig. 4) for mounting the load introductions which were connecting the nose cap with the vehicle's aluminium substructure. The C/C-SiC anchor attachments and pressure port plugs were joined to the nose cap shell by using a special in-situ technique which is an integrated step in the manufacturing process. The thin interface layer which connects both CMC parts is consisting of SiC and no carbon fibres are passing through. During the flight, the mechanical loads would be transferred through these interfaces and so one of the pivotal questions was: is the bonding quality of the interface layer sufficient? For this specific task the nose cap structure with its potentially

[1)] ROI = region of interest

failure critical joining interfaces was inspected within a medical CT facility at a hospital near the city of Heilbronn (Fig. 4). Figure 5 shows one of several hundred two-dimensional CT cross sections of the nose cap structure with two of the CMC load introduction clamps. The dashed section marks the region which is shown in a close up view beside (Fig. 6).

Fig. 3. DLR's C/C-SiC structure mounted on the nose tip of the X-38 vehicle (Johnson Space Center, Houston, TX)

Fig. 4. C/C-SiC nose cap structure during inspection in a medical CT facility (Klinikum Heilbronn, Germany)

Due to the fact that the 140 kV X-ray tube of the medical CT (Somatom Plus 4) is not designed for high resolution investigation, the characteristic microstructure of the C/C-SiC composite is not visible. However, the close up view of the joining layer area shows that the interface bonding is obviously sufficient and that there is no gap or delamination detectable. The two black "triangles" are cross-sections through interstitial spaces, induced by the curved laminate structure of the CMC clamps. It is no indication for structural defects. All CMC attachments (load introduction clamps and pressure port plugs) were thoroughly inspected that way. Although it was not possible to obtain high resolution images of the C/C-SiC microstructure, it was found that the joining interfaces were of sufficient quality for the flight.

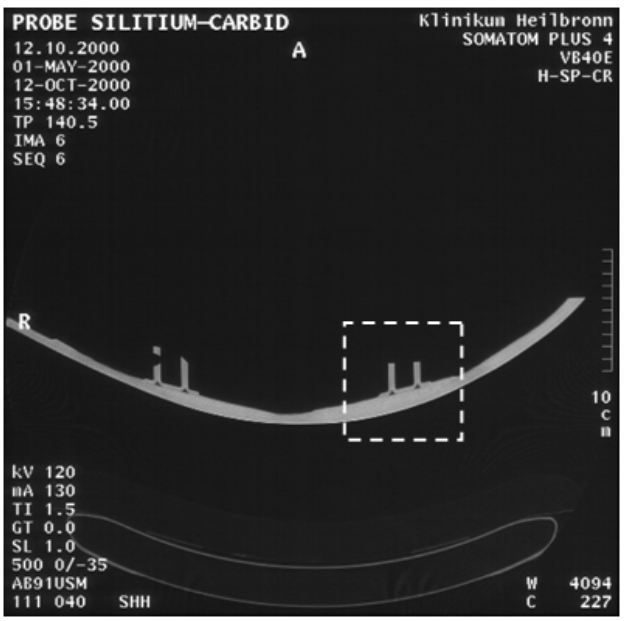

Fig. 5. Two-dimensional CT cross section of the complete X-38 nose cap structure with marked ROI (dashed square)

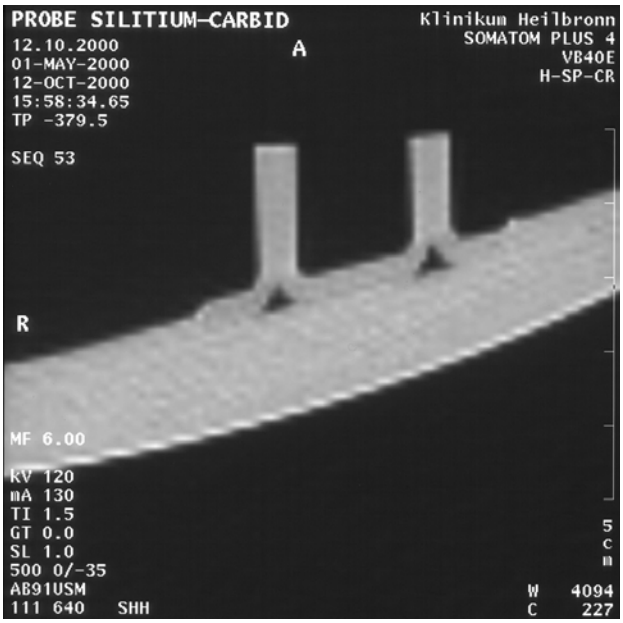

Fig. 6. Close up view of a load introduction attachment of the CMC nose cap structure (CT cross section)

Inspecting the Microstructure of CMC Components

With the development of EXPERT's CMC nose cap structure another design for the load introduction was favoured. The C/C-SiC nose cap is approximately 700 mm in diameter (Fig. 7). It is attached to the substructure with 16 load introductions and the so called C/C-SiC hat profiles are the anchorage points that are joined to the interior side of the

CMC nose cap shell (Fig. 8). The joining technique is the same as used for the CMC clamps of X-38. After pyrolizing the shell and the hat profiles separately, the hat profiles are glued on to the inside of the nose cap with a carbon rich phenolic resin. During siliconization above 1700 °C in argon atmosphere, the carbon-resin mixture is pyrolized and infiltrated by liquid silicon which then transforms to silicon carbide. Like with the joining layers of X-38, there are no carbon fibres which are passing through these interfaces. Thus, it is necessary to inspect the degree of homogeneity of the thin SiC joining interfaces and therefore to evaluate the bonding quality of these failure critical areas.

Fig. 7. EXPERT's C/C-SiC nose cap structure during a shaker test at ESTEC (Noordwijk, NL)

Fig. 8. Inside view of the nose cap structure with the CMC hat profile attachments as part of the 16 load introductions

With respect to the structure component's size, it has to be considered that the non-destructive inspection technique which will be used for qualifying flight hardware must allow detailed investigation of relatively confined regions which are located at almost inaccessible areas. As shown in Figure 9 and 10, the CT inspection facilities of DLR are fulfilling this demand. Figure 9 shows a three-dimensional false colour view of the complete nose cap's load introduction rim. This image is a calculated three-dimensional reconstruction of more than 4000 two-dimensional X-ray projections. Each of the visible C/C-SiC hat profiles was inspected separately with much higher resolution. In contrast to the very first CT investigations with the nose cap structure of X-38 some years before (Fig. 5 and 6), it is now possible to obtain detailed insight in the laminate's microstructure and the in-plane porosity distribution of the SiC joining interface. Previous work with the nanotome CT facility has shown that it is even possible to inspect the microstructure of cracks and to pay attention to single carbon fibre filaments [4]. Figure 12 shows the porosity within a hat profile's joining interface.

Fig. 9. 3-dimensional CT image, showing a part of the EXPERT nose cap structure with the CMC hat profiles

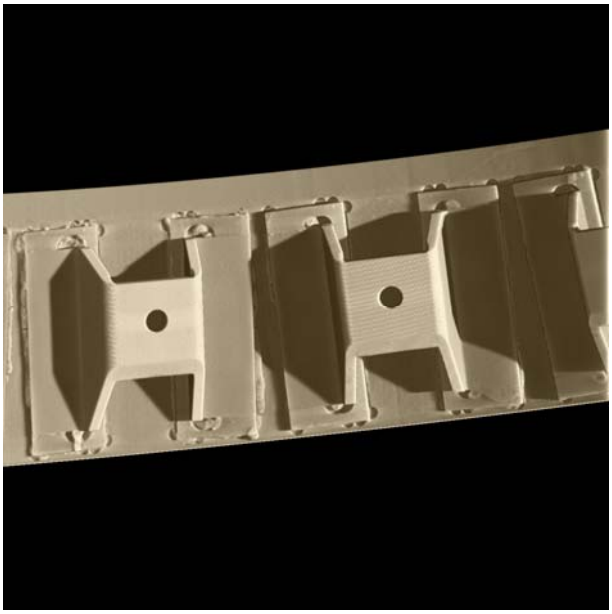

Fig. 10. 3-dimensional CT image with a close up view on some of the CMC hat profiles

As the cross-section in the left image of Figure 12 shows very clear, regions of higher porosity or even debonded areas can be easily detected (compare to Fig. 6). The following examples which are supposed to demonstrate the full potential of CT inspection tools were performed with a batch of mechanical qualification test dummies of the CMC hat profile geometry (Fig. 11). These test dummies were identical in shape and size compared to those attached to the C/C-SiC nose cap. The only difference is the shape of the dummy's base plate (representing the shell) which is plane instead of being slightly curved as with the real nose cap shell. The mechanical test assembly itself is shown in Figure 16 and some conclusions between microstructural aspects and observed failure modes are drawn in the following main chapter.

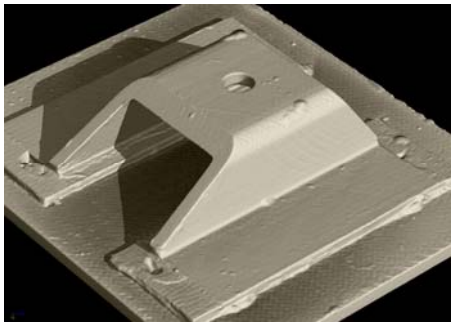

Fig. 11. 3-dimensional CT image of a single CMC hat profile demonstrator

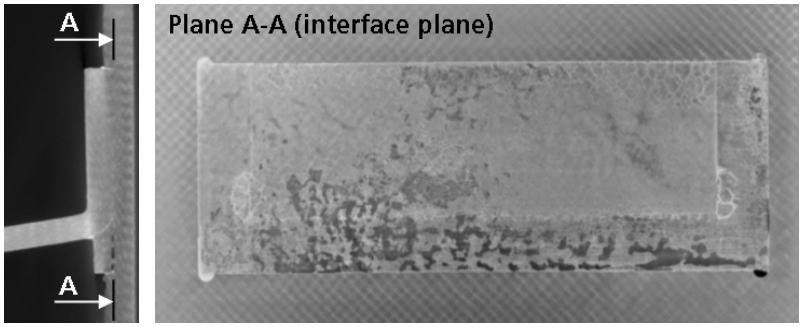

Fig. 12. 2-dimesional CT images with close up views on the joining interface between the nose cap and the attached CMC hat profile

Available Analysis Tools

As already shown, detailed CT investigations on structure components are capable to detect porosities within thin CMC joining layers. After data acquisition and reconstruction, the three-dimensional data set of voxels will be spatialized and pictured by a three-dimensional imaging software named VG Studio Max (version 2.0). Here it is possible to attribute a colour index to the detectable porosity size ranges which is defined by the average pore diameter [mm³]. As a result, Figure 13 shows the three-dimensional porosity distribution (0-120 mm³) – ordered and indexed by coloured pore size classes – within the two joining layers of a CMC hat profile. The statistical parameters of the pore size distribution are essential for a systematic evaluation of the joining layer's quality.

Beside the information of internal microstructural features of the CMC component, it is also important to collect data of the exterior shape and geometrical tolerances. Figure 14 shows a colour indexed image of the CMC hat profile which is indicating measurable variations of the wall thickness. For setting the tolerance range, three reference points were chosen. The coloured surfaces are indicating to what extend the wall thicknesses are differing according to these reference points. The grey surface colour is indicating, that this area is outside the wall thickness tolerance range.

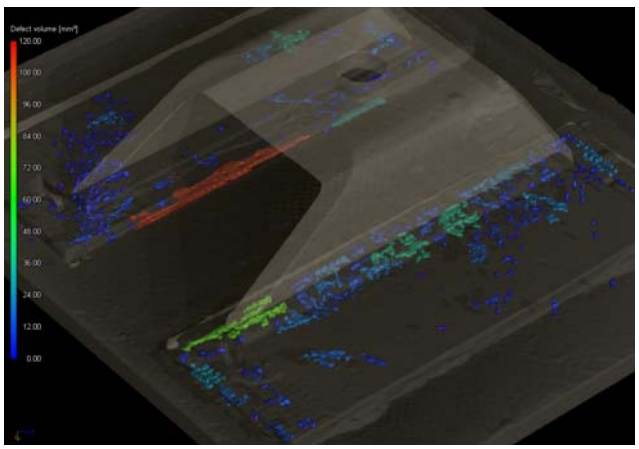

Fig. 13. Porosity size and distribution within the joining interface (pore size: 0-120 mm^3)

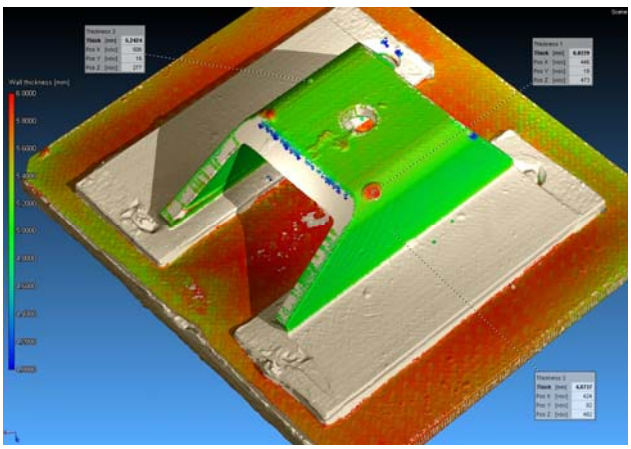

Fig. 14. Wall thickness analysis within a predefined tolerance interval (3 reference points; $\Delta = 2$ mm)

In terms of reverse engineering it is important to perform a set-actual analysis. After aligning the original CAD data set with the measured CT-based surface body, it is possible to evaluate the dimensional stability of the CMC structure component. The coloured image in Figure 15 shows a set-actual comparison of the CMC hat profile. Using a CAD reference, computed tomography offers the opportunity to evaluate and quantify any morphological mismatch of a real component and the original CAD geometry model. Compared to a three-dimensional coordinate measurement machine, a set-actual comparison via computed tomography also comprises surfaces which are not accessible from outside.

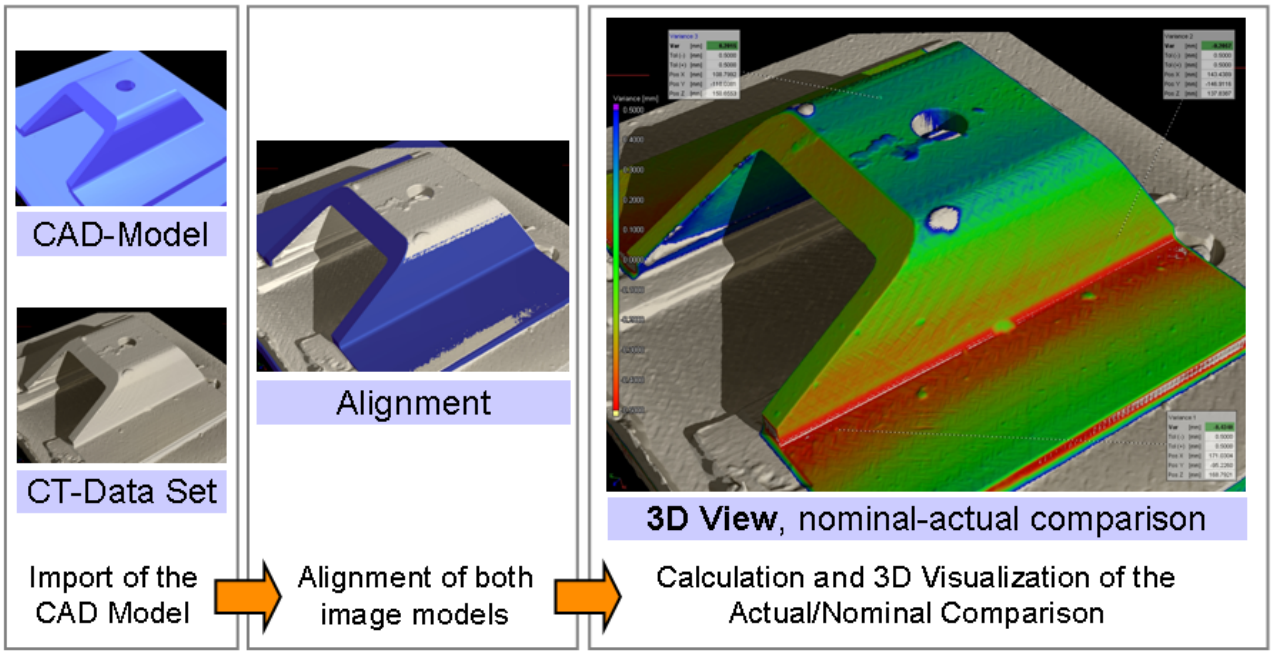

Fig. 15. Set-actual analysis between the CT scan and the CAD reference

COMPARISON OF CT ANALYSIS AND MECHANICAL TESTING DATA

As part of the qualification test programme for the EXPERT nose cap structure, 32 C/C-SiC hat profiles were produced for experimental testing. The specimens were differing by the type of C/C-SiC material and the carbon fibre orientation. All of them were inspected by microfocus CT and then tested under mechanical load in order to admit the optimum material combination/fibre orientation and to proof that the load introduction structure concept in general is appropriate for the expected shear forces that will occur during the flight. Figure 16 is showing the test assembly. The lower part with the C/C-SiC hat profile was fixed whereas the upper part was moving in a perpendicular direction as indicated by the axial force vector $\vec{F}$ (Fig. 16). As a result, two characteristic failure types were observed: a debonding of the joining interface between the CMC base plate (nose cap) or cracking due to bearing stresses within the attached CMC hat profile which is part of the load introduction itself. It was always either the debonding (Fig. 17) or the generation of microcracks (Fig. 18) which was observed as indication of mechanical failure. In total 14 specimens with comparable fibre orientation and similar CMC material type were selected for a more detailed CT investigation (voxel size: approx. 100 µm). The quality of the SiC interface layer by means of porosity was evaluated and compared to the maximum mechanical load and the resulting failure type. For a first qualitative evaluation of the bonding layer, a simple key was used for the CT inspection: (+) = good bonding quality – the interface shows no porosity at all (Fig. 19), (○) = medium bonding quality – the interface shows only few pores (Fig. 20) and (–) = low bonding quality – the interface shows widespread areas with porous structure (Fig. 21).

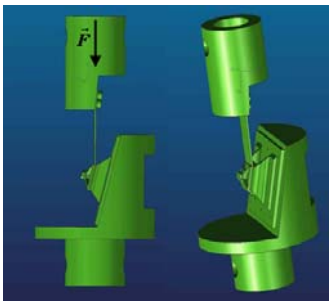

Fig. 16. Mechanical test device for the load introduction concept

Fig. 17. Mechanical failure by debonding within the joining interface

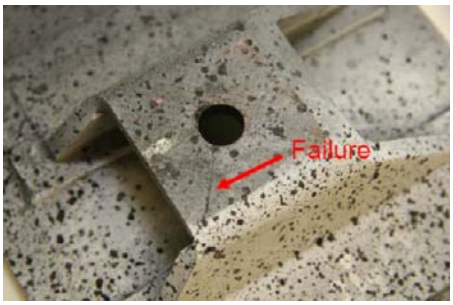

Fig. 18. Mechanical failure within the CMC material (cracking)

From a first comparison between the CT image analysis of the interface layers (Fig. 19-21) and the failure type (Fig. 17 and 18) that was observed as a result of the mechanical test of each specimen, it becomes obvious that the mechanical failure must be in connection with the degree of porosity and the porosity distribution within the bonding respectively. A high quality of the interface layer – which means that there is no porosity detectable at all – leads to a failure type of

crack formation within the CMC hat profile. Among all inspected specimens there was only one exception with hat profile #24-2: here a significant amount of porosity was detected with µ-CT which was the reason why the joining of this specimen was classified as a "poor quality" bonding. However, in this single case the mechanical failure occurred as a formation of microcracks within the hat profile. This exception cannot be explained so far but for all other 13 specimens the tendency was clear as those with poor and medium bonding quality were always showing debonding failure within the interface layer of the joining while those with good quality bonding showed failure cracks within the CMC material of the hat profile just as shown in Figure 18. That means that for the given design and load case, a high quality bonding layer can withstand higher loads than the CMC material of the hat profile.

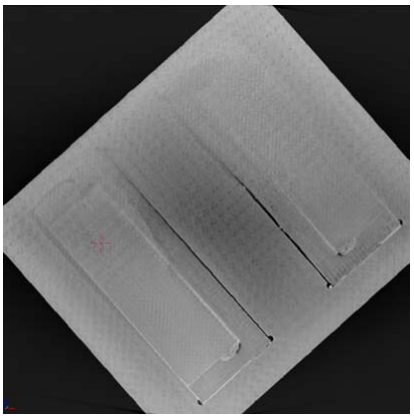

Fig. 19. Good quality of the interface bonding layer (+)

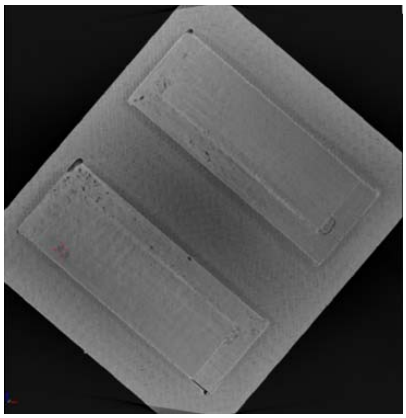

Fig. 20. Medium quality of the interface bonding layer (○)

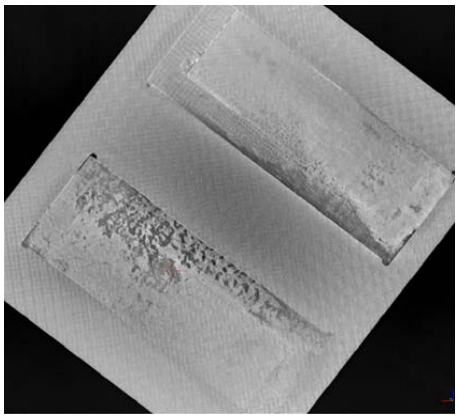

Fig. 21. Poor quality of the interface bonding layer (–)

The failure load of each demonstrator was determined with the mechanical tests. Though the measurement values show significant dispersion, it seems obvious that with higher porosity of the joining interface the absolute failure load value is slightly decreasing. Figure 22 shows the average failure loads as ordered by bonding quality.

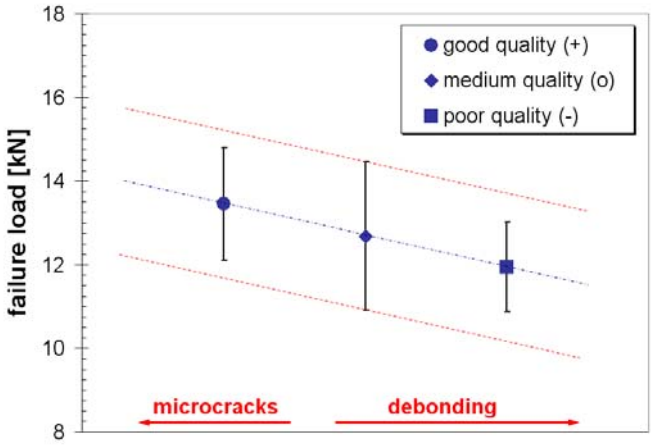

Fig. 22. Failure loads versus bonding layer quality classification

As indicated by the failure bars, the average failure loads show some degree of deviation which superimposes the tendency of decreasing values with diminishing bonding quality. This is the main reason why it is still so difficult to quantify the numerical coherence between the interface porosity and the failure load. The main obstacle is certainly the lack of an established knowledge base for the classification and validation for the assessment of the joining interface layer which would help to quantify the state of quality. This problem is going to be addressed in the near future by developing quantitative and statistical evaluation methods for detailed CT investigations on monitoring pore sizes, volumes and distribution within a joining interface layer.

CROSS-LINKING CT ANALYSIS DATA AND NUMERICAL SIMULATION

Figure 16 shows that the orientation of the load introduction (axial force vector $\vec{F}$) is not exactly parallel to the bonding layer. That is why the first separation of most debonded specimens appears at the upper region of the interface bonding layer (Fig. 17). From this point it seems quite clear that in terms of structural stability of the load introduction in general and the bonding quality in particular, is not only a question of the amount of porosity and the statistical pore size

distribution but the absolute position of porosity within the joining interface. This aspect can only be considered in detail by additionally integrating CT analysis data into numerical modelling. The Figures 23 and 24 below are showing a 3-point bending test specimen of C/C-SiC material which is partially delaminated. The image data is based on a high resolution CT scan which was obtained by the µ-CT facility. After reconstruction of the specimen's volume data set, all structural features were meshed by using special software modules in order to import the information into numerical modelling. Other authors were following a similar strategy before [5-7].

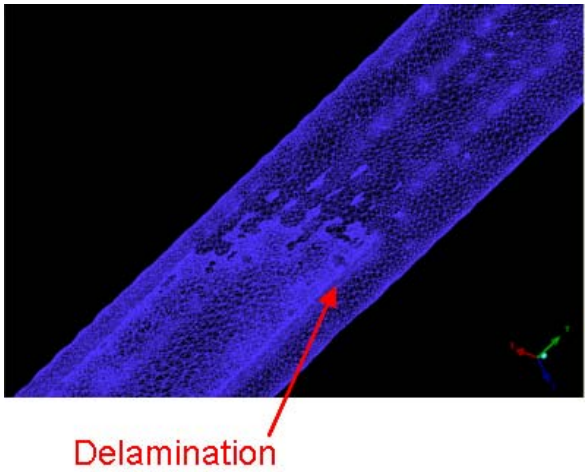

Fig. 23. Three-dimensional view of a C/C-SiC bending test sample with a delamination defect (based on CT data)

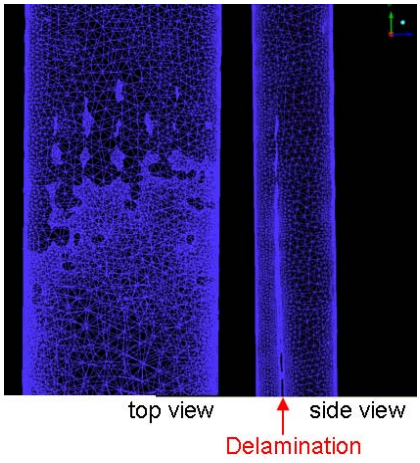

Fig. 24. Two-dimensional views of the detected delamination defect

CONCLUSIONS

Computed tomography is a powerful tool for non-destructive inspection that allows the performance of a bunch of interesting and useful investigations on structural CMC components. With no other technique it is possible to identify such small structural features and defects in failure critical areas of a large structure component. Beside the capability of detecting and imaging defects, it is very important to establish new measurement procedures for obtaining quantitative parameters and comprehensive statistical evaluation. Reliable failure mode and life time prediction will only be possible if the full three-dimensional information content of a CT data set from experimental testing can be transferred to numerical modelling. With finite-element analysis that is also based on CT data obtained by investigations from experimental test testing, the significance and reliability of existing numerical models could be improved decisively.

ACKNOWLEDGMENT

The authors wish to express their gratitude to Prof. Dr. med. Peter Prager, who – as head of the Department for Nuclear Medicine and Radiology, Klinikum Heilbronn, Germany – made it possible to use the hospital's medical CT facility for inspections on the X-38 nose cap structure. And for the young team of radiologists there, please accept our best thanks for supporting us during the CT measurement procedures.

REFERENCES

[1] H. Hald, H. Weihs, B. Benitsch, I. Fischer, T. Reimer, P. Winkelmann, A. Gülhan, "Development of a CMC nose cap system for X-38," Proceedings of the International Symposium on Atmospheric Reentry Vehicles and Systems, 16-18 March 1999, Arcachon, France, published on CD.

[2] H. Hald, H. Weihs, "Safety Aspects of CMC Materials and Hot Structures," *Joint ESA-NASA Space Flight Safety Conference*, ESA-SP-486 (2002), pp. 127-133.

[3] W. Krenkel, J. Fabig, "Tailoring of Microstructure in C/C-SiC Composites," Proceedings of ICCM-10 (1995), Vol. IV, pp. 601-609.

[4] T. Ullmann, R. Jemmali, S. Hofmann, "Non-Destructive Evaluation Methods for CMC Components," Proceedings of ICACC-2009, by the American Ceramic Society, 19-23 Jan. 2009, Daytona Beach, FL, to be published.

[5] A. Abdul-Aziz, J. Downey, L.J. Ghosn, G.Y. Baaklini, "A CAD Approach to Integrating NDE with Finite Element," NASA/TM-2004-212904 (2004), 23 pages, available at: http://gltrs.grc.nasa.gov

[6] A. Abdul-Aziz, C. Saury, V. Bui Xuan, P. Young, "On the Material Characterization of a Composite using Micro CT Image based Finite Element Modeling," Proceedings of SPIE, Vol. 6176 (2006), pp. 32-39.

[7] I.G. Watson, P.D. Lee, R.J. Dashwood, P. Young, "Simulation of the Mechanical Properties of an Aluminum Matrix Composite using X-ray Microtomography," *Metallurgical and Materials Transactions A*, 37A (2006), pp. 551-558.